

Controlled growth of ZnO nanorod templates and TiO₂ nanotube arrays by using porous TiO₂ film as mask

Jijun Qiu · Weidong Yu · Xiangdong Gao · Xiaomin Li · Weizhen He ·
Se-Jeong Park · Hyung-Kook Kim · Yong-Hwae Hwang

Received: 23 January 2008 / Accepted: 13 May 2008 / Published online: 3 June 2008
© Springer Science+Business Media, LLC 2008

Abstract Porous TiO₂ thin films obtained from sol–gel self-organize approach were firstly used as masks to control the growth of ZnO nanorod arrays by aqueous solution method. The effect of TiO₂ pore size on the density of ZnO nanorod arrays was investigated by atomic force microscopy and field emission scanning electron microscope. The results show that the density of ZnO nanorod arrays obviously decreases after using porous TiO₂ masks, and increases with increasing the TiO₂ pore size. Additionally, the existence of TiO₂ mask can also effectively prolong the wet-chemical etching time of TiO₂ nanotube arrays manufactured from ZnO nanorod templates assisted sol–gel method, to completely remove the ZnO nanorod templates and to avoid collapsing of TiO₂ nanotube arrays from the substrates.

Keywords ZnO nanorod arrays · Porous TiO₂ thin films · Mask · TiO₂ nanotube arrays · Sol–gel self-organize

J. Qiu (✉) · W. Yu · X. Gao · X. Li
State Key Laboratory of High Performance Ceramics
and Superfine Microstructures, Shanghai Institute of Ceramics,
Chinese Academy of Sciences, No.1295, Dingxi Road,
Shanghai 200050, People's Republic of China
e-mail: jj_qiu@163.com

J. Qiu
RCDAMP, Pusan National University, Busn 609-735,
South Korea

W. He · S.-J. Park
Department of Nano Fusion Technology,
Pusan National University, Miryang 627-706, South Koera

H.-K. Kim · Y.-H. Hwang
Department of Nanomaterials & BK 21 Nano Fusion
Technology Division, Pusan National University,
Miryang 627-706, South Koera

1 Introduction

Due to high surface-to-volume ratios, excellent mechanical, optical and electronic transport properties in comparison with colloid, powder and film materials, one dimensional (1D) TiO₂ nanotubes are promising candidate for applications in photocatalysts [1], gas sensors [2], photovoltaic solar cells [3] and rechargeable lithium batteries [4]. Therefore, particular attention has been paid to the preparation of 1D TiO₂ nanotubes or nanotubal arrays, and many methods have been developed including electrochemical anodic oxidation of pure titanium sheet [5, 6], hydrothermal treatment of TiO₂ nanoparticles with alkali solution, hydrolysis of TiF₄ under acidic conditions [7], porous alumina (PA)—template methods [8, 9]. Up to date, however, oriented TiO₂ nanotube arrays directly grown on conductive substrates, which are often more desirable for applications employing the wide band-gap semiconductor, cannot be obtained from these methods. There is a requirement for the development of a facile and reproducible way to synthesize oriented TiO₂ nanotube arrays on the conductive substrate.

Recently, a significant progress was achieved by Yang [10] and Kim [11], who demonstrated that inorganic nanotubes can be obtained by using ZnO nanorods grown from the desired substrates as template. Their procedures are composed of ZnO template-inorganic coating core-shell formation and ZnO template removal procedure, which involves the use of catalysts, high temperature, and a vacuum technique, leading to increase the cost and to limit the choice of substrates. Subsequently, we had improved this procedure by selecting an environment friendly synthesis route with a low-temperature in common-pressure: aqueous solution growth method for ZnO nanorod arrays, sol–gel dip-coating technique for inorganic shell coating,

and wet-chemical route for removal of ZnO template [12–15]. In comparisons with other available growth techniques for 1D ZnO nanorods, for example, catalytic growth via the vapor–liquid–solid mechanisms [16], metal–organic chemical vapor deposition [17], vapor phase transport deposition [18], pulsed laser deposition [19] and epitaxial electrodeposition [20], aqueous solution method route has a good potential for scale-up production in low-cost. In contrast to other methods such as atom layer deposition [11], electrophoresis [21], liquid phase deposition [22], the unique advantages of the sol–gel dip-coating process are low processing temperature, low-cost, high purity and homogeneity, good shaping ability and easy fabrication of extremely light materials and porous materials. Therefore, ZnO nanorod template assisted with sol–gel dip-coating method has proven to be a versatile route to generate oriented TiO₂ nanotube arrays over large area on substrates.

In spite of a great deal of effort to successfully synthesize TiO₂ nanotube arrays on the substrates in our group, however, several barriers still exist due to the intrinsic properties of ZnO template obtained from aqueous solution method. Firstly, it is still a significant challenge to control the density and the orientation of ZnO template obtained from aqueous solution by an efficient and low-cost technique. Currently, lithography techniques [23–28], including photolithography, e-beam lithography, nanoimprint lithography, nanosphere lithography and mask lithography via porous alumina, generally are used to precisely control the position and the density of ZnO nanorods on the substrates, which involve high production costs for sophisticated equipment and power consumption. Second, well-aligned TiO₂ nanotube arrays with open-ended structure are only obtained for a narrow range of synthetic conditions, such as dip-coating number, wet-etching time and heating rate. For instance, it is necessary to increase the etching time to

completely eliminate ZnO template, however, an irreversible deterioration and collapse of TiO₂ nanotubes from the substrates is often associated with the elimination of the template in the wet-chemical etching procedure. This is due to that the ZnO seed layer, which are pre-deposited on the substrate for inducing the oriented growth of ZnO nanorods in aqueous solution process, also may be easily etched by wet-chemical etching solution when removing ZnO nanorod templates, leading to TiO₂ nanotubes deposited over it detaching from the substrates.

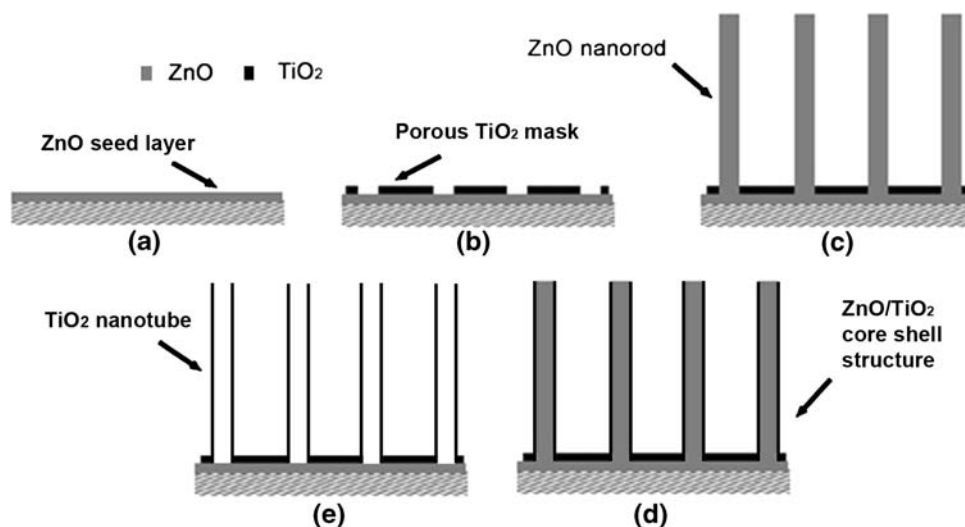
Herein we firstly proposed to use porous TiO₂ thin film as mask to control the density of ZnO nanorod template and to avoid the collapse of TiO₂ nanotube arrays from the substrates in the course of eliminating ZnO templates. The porous TiO₂ mask are formed by sol–gel self-organize technique [29, 30], which is a cheap, effective, and scalable to 10s of inches in linear dimension. By adjusting the size of TiO₂ pores, the density of well-aligned ZnO nanorod templates could be changed from 10¹⁰ to 10⁸ cm⁻². At the same time, TiO₂ mask deposited over the ZnO seed layer will prevent direct contacting between etching solution and the ZnO seeds to protect ZnO seed layer from etching, so we can increase the etching time to remove completely the ZnO nanorod templates and avoid the collapsing of inorganic nanotubes.

2 Experimental details

The whole fabrication process is illustrated schematically in Fig. 1.

First, ZnO seed layer was deposited on glass substrates from sol–gel method. Second, porous TiO₂ mask was deposited on the ZnO seed layer to control the density of ZnO seeds by coating some area of ZnO seed layer. In other

Fig. 1 Schematics of the fabrication process of TiO₂ nanotube arrays by ZnO nanorod templates assisted sol–gel technique. (a) Deposition of the ZnO seed layer by sol–gel method; (b) Deposition of the porous TiO₂ membrane on the ZnO seed layer by sol–gel self-organize approach; (c) Synthesis of ZnO nanorod templates by aqueous solution method; (d) Fabrication of ZnO–TiO₂ core-shell structures by dip-coating method; (e) Removing ZnO nanorod templates by wet-chemical solution



words, ZnO nanorods can only grow out from the TiO₂ pores where expose the ZnO seeds. Then aqueous solution method was used to manufacture the ZnO nanorods at low temperature (70 °C), and the fabrication process of TiO₂ nanotube arrays by sol–gel assisted ZnO nanorod templates was described in Ref. [9].

2.1 Deposition ZnO seed layer

Sol–gel method was used to obtain high quality ZnO seed layers. In brief, Zn(CH₃COO)₂ · 2H₂O (0.75 mol/L) was dissolved in a 2-methoxyethanol-monoethanolamine solution at room temperature. The resultant solution was stirred at 60 °C for 0.5 h to yield a clear and homogeneous solution. Then clean glass substrates (30 mm × 25 mm) were dipped into the sol, withdrawn at 3.0 cm min⁻¹ and dried at air. Then as-coated substrates were preheated at 300 °C for 10 min and then were heated up to 550 °C at a 2 °C/min for 1 h to obtain dense and transparent ZnO catalyst particle layers on glass substrates.

2.2 Deposition of porous TiO₂ membrane

The porous TiO₂ mask are formed by sol–gel self-organize technique. In brief, tetrabutylorthotitanate (TBT), alcohol (EtOH), deionized water (H₂O), diethanolamine (DEA), together with polyethylene glycol (PEG, the molecular weight is 1,000), which servers as porous structure-directing agent, were mixed with the molar ratio [n(TBT) : n(DEA) : n(H₂O) : n(PEG) : n(EtOH) = 1 : 1 : 1 : (0 ~ 0.05) : 26.5] to form a light yellow solution. After being stirred for 2 h, the light yellow solution was gelatinized for 24 h. Then the sol was deposited on ZnO seed layer coated substrates to form a wet gel by using the dip-coating method with a drawing speed of 2.0 cm/min at 60% relative humidity (RH). The wet film was dried at 100 °C for 10 min, and then was calcined at 550 °C for 1 h. To avoid cracks, the heating rate should be slow, about 2 °C/min.

2.3 Growth of ZnO nanorod templates by aqueous solution

Precursor aqueous solution was prepared by dissolving zinc nitrate hydrate (Zn(NO₃)₂ · 6H₂O) and alkali (NaOH) in deionized water. The concentration of zinc and alkali were fixed at 0.01 and 0.4 mol/L, respectively. ZnO-coated substrates were suspended in the precursor solutions at 70 °C for 25 min under strong stirring. Subsequently, the resultant films were thoroughly washed with deionized water to remove any residual salt or amino complex and dried in air at room temperature.

2.4 Preparation of TiO₂ nanotube arrays

Then TiO₂ sol without PEG obtained from process (2.2) was deposited on ZnO nanorod templates by dip-coating with a withdrawing speed about 0.5 cm/min. The deposited films were dried at 100 °C for 10 min, and heated up to 550 °C for 1 h at 2 °C/min in air to obtain crystalline ZnO/TiO₂ core-shell nanorod arrays. Subsequently, the ZnO/TiO₂ nanorod arrays were immersed in 3% (v/v %) diluted hydrochloric acid aqueous solution at room temperature for 15 ~ 120 s to remove ZnO nanorod templates and to obtain hollow TiO₂ nanotubes.

2.5 Characterization of samples

The crystallization and phase structure of ZnO catalyst seed layers were analyzed by an X-ray diffractometer (XRD: D/max 2200 PC with Cu Ka, Rigaku Co., Tokyo, Japan). The morphology of the surface and the fracture cross section of the specimens were observed by an atomic force microscopy (AFM: SPA 400) and a field emission scanning electron microscope (FESEM: S-4700, Hitachi).

3 Results and discussion

Figure 2 gives XRD pattern and AFM graph of the ZnO seed layer obtained from sol–gel. From Fig. 2a, only a (002) peak of ZnO is observed, showing that the ZnO seed is preferentially oriented along the c-axis direction. Figure 2b shows 5 × 5 μm² 3D AFM image of ZnO seed layer. It's clear that the film has a dense surface structure composed of regular grains with an average diameter of about 100 nm, and no visible pores and defects can be observed over the seed layer. The surface root-mean-square roughness (RSM) is about 3 nm and the maximum value of roughness is 10 nm, showing very smooth surface structure. The ZnO seed layer with the c-axis preferred orientation, good crystalline and smooth surface is favorable for the subsequent vertical growth of ZnO nanorod templates.

It is well known that the pore size and the density of porous TiO₂ thin films are quite sensitive to preparation conditions, such as composition, chemical additives, withdrawal speed and humidity. Figure 3 shows the AFM topography (5 × 5 μm² 2D) and accompanying profiles of the surface of porous TiO₂ thin films prepared from various amount of PEG (1000) at 60% RH with a withdrawal speed of 2 cm/min. There are many nanometer or sub-micrometer pores produced in the TiO₂ films, resulting from decomposing of PEG at 550 °C. The pore size and density are related to the PEG (1,000) concentration in TiO₂ sol. As increasing the PEG concentration from 0.01 to 0.05, the

Fig. 2 XRD pattern and AFM image of ZnO seed layer coated glass substrate. (a) XRD pattern; (b) 3D-AFM image

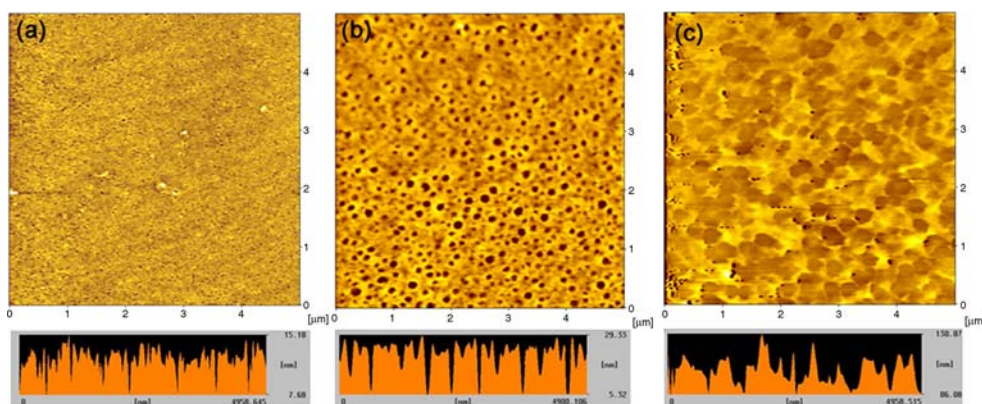
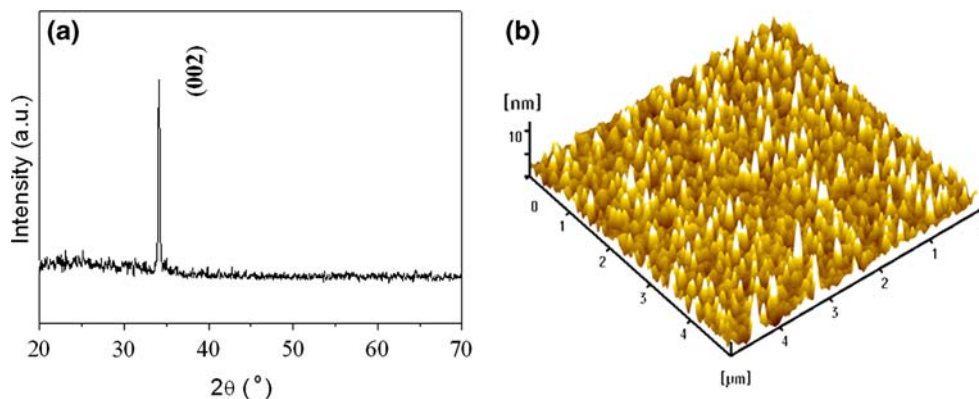


Fig. 3 AFM images and accompanying profiles of porous TiO₂ masks obtained from various PEG concentrations. (a) 0.01; (b) 0.03; (c) 0.05

diameter and the depth of TiO₂ pores increase from ~ 20 to ~ 250 nm and from ~ 8 to ~ 44 nm, respectively, and the pore density decreases from $\sim 1.6 \times 10^{11}$ to $\sim 3.2 \times 10^8$ cm⁻². This is ascribed to the fact that with an increase in the amount of PEG in TiO₂ sol, the viscosity increases and more polymerization-induced phase separation occurs at earlier stages in the growth process of TiO₂, and earlier phase separation leads the system to lower volume fraction of polymerizing TiO₂ clusters [18].

Figure 4 shows the related XRD pattern of porous TiO₂ mask deposited on the ZnO seed layers. It is clear that except for ZnO (002) peak at 34.4°, a new peak can be observed at 25.4°, assigning to (101) diffraction peak of anatase TiO₂ (JCPDS no. 21-1272). This result indicates porous TiO₂ masks obtained from PEG assisted sol-gel may be predominantly oriented along the $\langle 101 \rangle$ direction on ZnO seed layers. Additionally, the intensity of TiO₂ (101) peak doesn't degenerate with increasing the PEG concentration, meaning the PEG concentration has little influence over the crystallization of TiO₂ mask.

Figure 5a shows the ZnO nanorod templates directly grown from ZnO seed layer without the porous TiO₂ membranes. It is clear that all ZnO seeds were completely utilized to induce the vertical growth of ZnO nanorods,

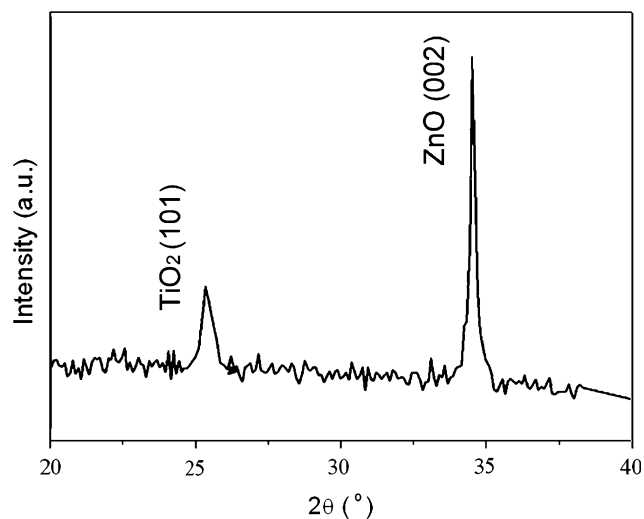
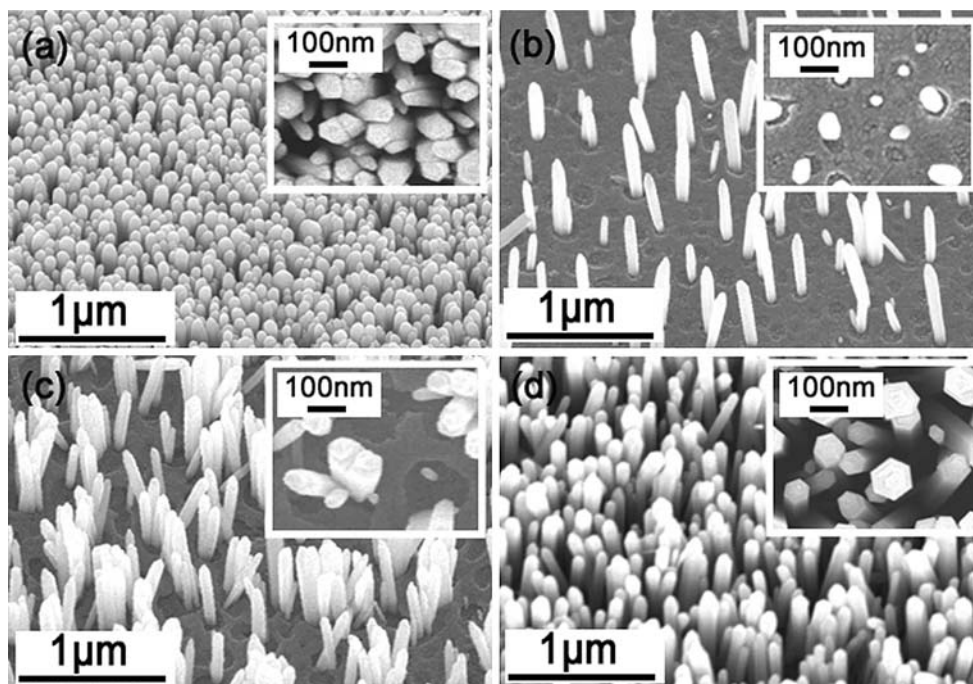


Fig. 4 XRD pattern of TiO₂ mask deposited on the ZnO seed layer, which was synthesized from 0.03 M PEG

resulting in high density of 2.5×10^{10} cm⁻². Figure 5b–d shows the FESEM images of ZnO nanorod templates grown out from porous TiO₂ masks. It is obvious that the density of ZnO nanorod templates grown from porous TiO₂ masks distinctly decreases. Although the pore density

Fig. 5 Tilted 25° and plan-view FESEM images (inset) of ZnO nanorod templates grown from porous TiO₂ masks with various pore size and density obtained from various PEG concentrations; (a) Directly grown on catalyst particle layer-coated glass substrate; (b) 0.01; (c) 0.03; (d) 0.05



decreases with increasing PEG concentration from 0.01 to 0.05, the density of ZnO nanorods increases from 4×10^8 to $5 \times 10^9 \text{ cm}^{-2}$, indicating that pore size has more significant effect on the density of ZnO nanorods. Only individual ZnO nanorod can grow from a small size TiO₂ pore, as shown in Fig. 5b, two and more ZnO nanorods can grow from a bigger TiO₂ pore size obtained from relatively higher PEG concentration. It should be noticed that the density of ZnO nanorods grown from the TiO₂ mask obtained from 0.01 PEG concentration is less than the pore density of the TiO₂ mask, meaning that not every TiO₂ pore can grow ZnO nanorod. We think that it is only through-TiO₂ pore extended into ZnO seed layer that grow ZnO nanorod.

As the ZnO nanorod arrays are used as template to fabricate the TiO₂ nanotube arrays, TiO₂ nanotube arrays can inherit the structural features of ZnO nanorod array template, such as the hexagonal shape, the length, the diameter and the density. So we can control the preparation of ZnO nanorod templates to achieve controlled growth of

TiO₂ nanotube arrays. Figure 6 shows representative FESEM images of TiO₂ nanotube arrays with various densities, which were fabricated from ZnO nanorod templates grown from porous TiO₂ masks with various pore sizes. Therefore, it is a simple route to control the density of TiO₂ nanotube arrays by depositing porous TiO₂ thin film with tunable pore sizes over the ZnO seed layer.

In the fabrication process of TiO₂ nanotube arrays by sol-gel assisted ZnO nanorod template, the etching time is very important to form hollow structure. In the case of shorter etching time, ZnO nanorod templates can't be completely removed and can't obtain hollow TiO₂ nanotubes, as shown in Fig. 7a. In order to obtain completely hollow TiO₂ nanotube arrays grown on the substrates, it is necessary to prolong the etching time. Unfortunately, increasing the etching time, the ZnO seed layer can also be etched by etching liquid, resulting in peeling TiO₂ nanotubes off from the substrate, as shown in Fig. 7b. However, after being deposited over the ZnO seed layer, porous TiO₂ thin film can protect the ZnO seed layer from being

Fig. 6 Plan-view FESEM images of TiO₂ nanotube arrays fabricated from different density ZnO nanorod templates grown from various TiO₂ masks. (a) 0.01; (b) 0.03; (c) 0.05

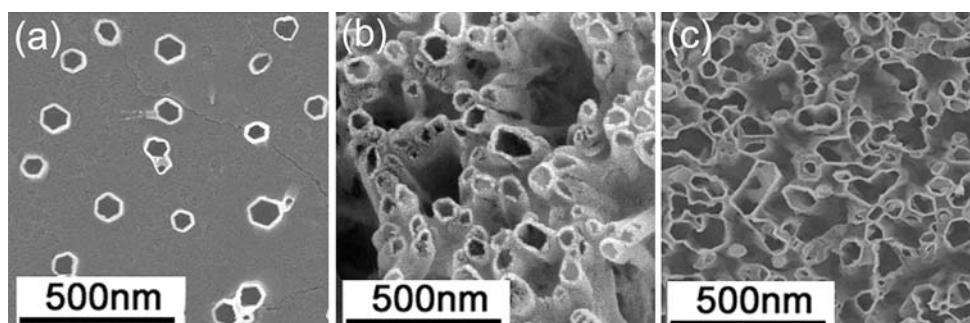
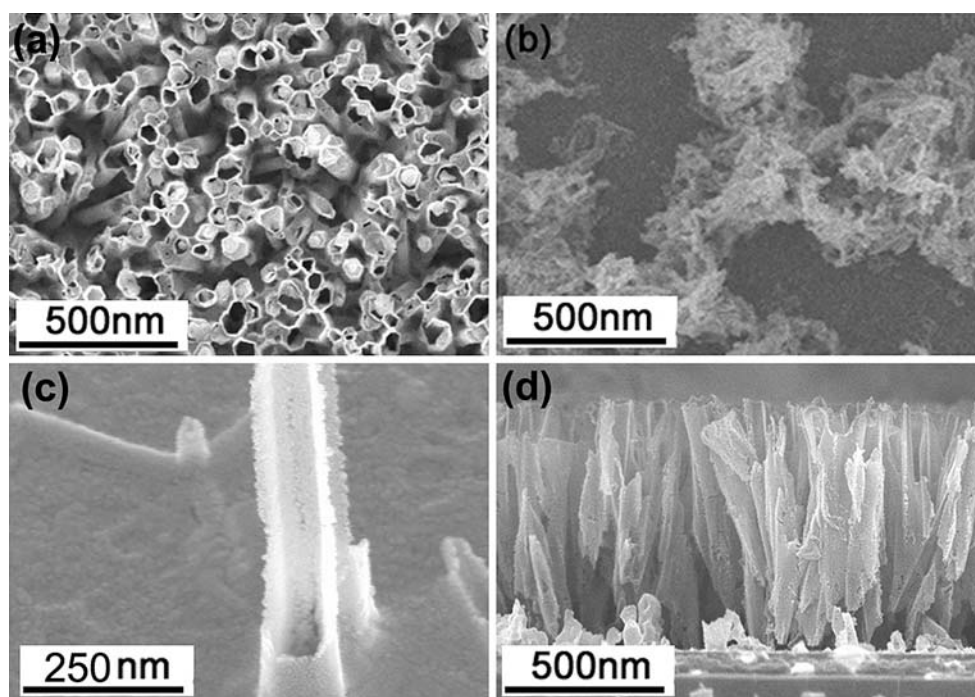


Fig. 7 Effects of etching time and porous TiO₂ masks on the morphology of TiO₂ nanotube arrays. (a) 15 s without TiO₂ masks; (b) 60 s without TiO₂ masks; (c) and (d) 60 s with TiO₂ mask



destroyed by preventing the etching solution eroding the ZnO seed layer. So we can increase the etching time from 15 to 120 s to completely remove the ZnO nanorod templates. It can be seen from their cross-sectional view images showing in Fig. 7c and d that ZnO nanorod templates at bottom of TiO₂ nanotubes completely disappear and the TiO₂ nanotubes vertically stand on the substrate as the etching time is above about 60 s.

4 Conclusions

In summary, porous TiO₂ thin films obtained from sol–gel method were successfully used as mask to control the density of ZnO nanorod obtained from aqueous method and TiO₂ nanotube arrays synthesized by ZnO nanorod templates assisted sol–gel method. The AFM images show that the size of TiO₂ pore obviously increases from 20 to 250 nm and the pore density decreases from $\sim 1.6 \times 10^{11}$ to $\sim 3.2 \times 10^8 \text{ cm}^{-2}$ with increasing the PEG concentration from 0.01 to 0.05. After the porous TiO₂ masks with various pore sizes were deposited over the ZnO seed layers, the density of ZnO nanorods decreases from 10^{10} to 10^8 cm^{-2} . However, the density of ZnO nanorods increases with increasing the size of TiO₂ pore, this is due to that two and more ZnO nanorods can grow from a bigger size TiO₂ pore. Except for controlling the density of ZnO nanorod templates, porous TiO₂ masks also can avoid breaking away TiO₂ nanotubes obtained from sol–gel assisted ZnO nanorods template in the case of longer etching time, by preventing etching liquid eroding ZnO seed layers. With

increasing the etching time, ZnO nanorod templates can be completely remove to achieve hollow nanotubal structure.

Acknowledgements This project was financially supported by National Natural Science Foundation of China (NSFC No. 50302013 and 50502038), Shanghai Natural Science Foundation (05ZR14132), and Shanghai Applied Materials Research and Development Fund (06SA07).

References

1. Chu SZ, Inoue S, Wada K, Li D, Haneda H, Awatsu S (2003) *J Phys Chem B* 107:6586
2. Varghese OK, Gong DW, Paulose M, Ong KG, Dickey EC, Grimes CA (2003) *Adv Mater* 15:624
3. Wei MD, Konishi Y, Zhou HS, Yanagida M, Sugihara H, Arakawa H (2006) *J Mater Chem* 16:1287
4. Zhou HS, Li DL, Hibino M, Honma I (2005) *Angew Chem Int Ed* 44:797
5. Mor GK, Varghese OK, Paulose M, Mukherjee N, Grimes CA (2003) *J Mater Res* 18:2588
6. Varghese OK, Mor GK, Grimes CA, Paulose M, Mukherjee N (2004) *J Nanosci Nanotechnol* 4:733
7. Liu SM, Gan LM, Liu LH, Zhang WD, Zeng HC (2002) *Chem Mater* 14:1391
8. Lee S, Jeon C, Park Y (2004) *Chem Mater* 16:4292
9. Park I, Jang S, Hong J, Vittal R, Kim K (2003) *Chem Mater* 15:4633
10. Goldberger J, He R, Lee S, Zhang Y, Yan H, Choi H, Yang P (2003) *Nature* 422:599
11. Hwang J, Min B, Lee JS, Keem K, Cho K, Sung MY, Lee MS, Kim S (2004) *Adv Mater* 16:422
12. Qiu JJ, Yu WD, Gao XD, Li XM (2006) *Nanotechnology* 17:4695
13. Qiu JJ, Yu WD, Gao XD, Li XM (2006) *Nanotechnology* 18:295604

14. Qiu JJ, Yu WD, Gao XD, Li XM (2007) *J Sol-Gel Sci Technol* 44:235
15. Qiu JJ, Jin ZG, Liu ZF, Liu GQ, Wu WB, Zhang X, Gao XD (2007) *Thin Solid Films* 515:2897
16. Huang H, Wu Y, Feick H, Tran N, Webe E, Yang P (2001) *Adv Mater* 13:113
17. Baxter JB, Aydil ES (2005) *J Cryst Growth* 274:407
18. Liu DF, Xiang YJ, Liao Q, Zhang JP, Wu XC, Zhang ZX, Liu LF, Ma W, Shen JJ, Zhou WY, Xie SS (2007) *Nanotechnology* 18:405303
19. Sun Y, Fuge GM, Ashfold MNR (2004) *Chem Phys Lett* 396:21
20. Liu R, Vertegel AA, Bohannon EW, Sorenson TA, Switzer JA (2001) *Chem Mater* 13:508
21. Limmer SJ, Hubler TL, Cao C (2003) *J Sol-Gel Sci Technol* 26:577
22. Dutschke A, Diegelmann C, Löbmann P (2003) *J Mater Chem* 13:1058
23. Ng HT, Han J, Yamada T, Nguyen P, Chen YP, Meyyappan M (2004) *Nano Lett* 4:1247
24. Park JW, Kim JK, Suh KY (2006) *Nanotechnology* 17:2631
25. Fan HJ, Fuhrmann B, Scholza R, Syrowatka F, Dadgar A, Krost A, Zacharias M (2006) *J Cryst Growth* 287:34
26. Wang X, Summers CJ, Wang ZL (2004) *Nano Lett* 4:423
27. Rybczynski J, Banerjee D, Kosiorek A, Giersig M, Ren ZF (2004) *Nano Lett* 4:20379
28. Banerjee D, Rybczynski J, Huang JY, Wang DZ, Dempa D, Ren ZF (2005) *Appl Phys. A* 80:749
29. Yu J, Yu JC, Cheng B, Zhao X, Zheng Z, Li ASK (2002) *J Sol-Gel Sci Technol* 24:229
30. Bu SJ, Jin ZG, Liu XX (2004) *J Sol-Gel Sci Technol* 30:241